

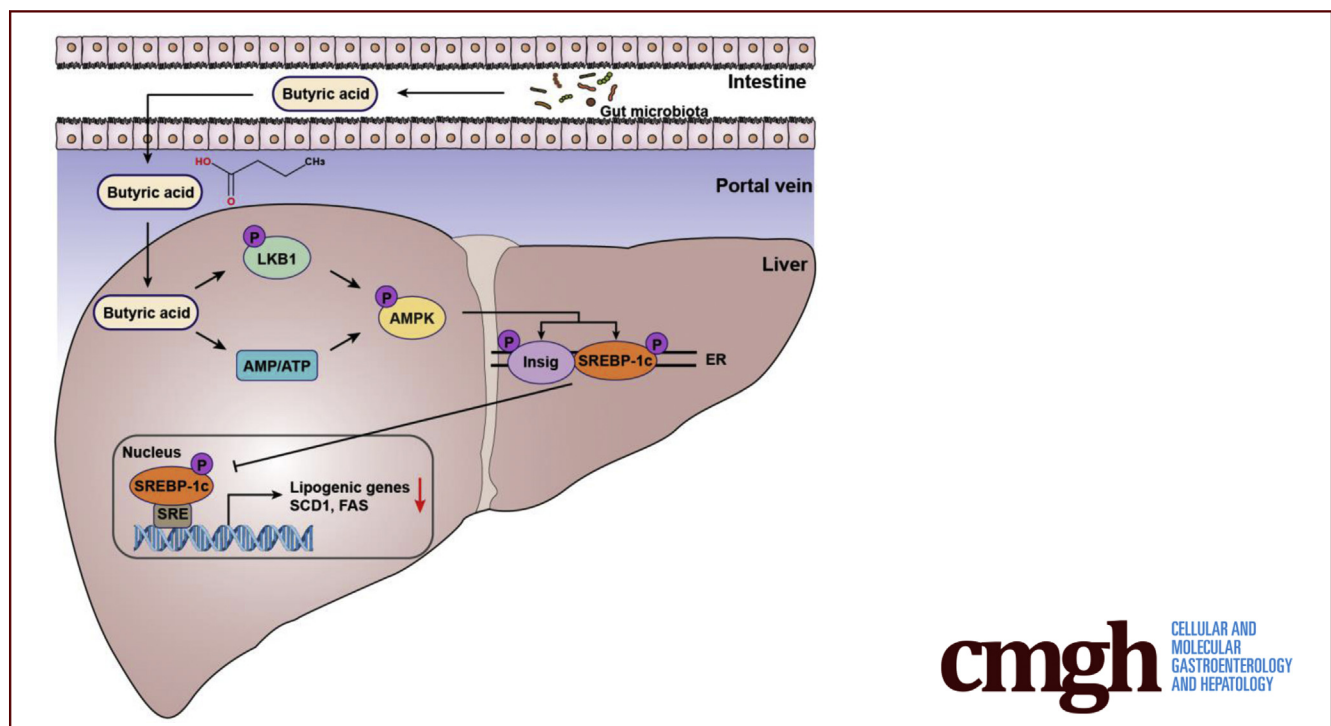
## ORIGINAL RESEARCH

## Sodium Butyrate Supplementation Inhibits Hepatic Steatosis by Stimulating Liver Kinase B1 and Insulin-Induced Gene



Ze-Hua Zhao,<sup>1,2,\*</sup> Zi-Xuan Wang,<sup>1,\*</sup> Da Zhou,<sup>1,3</sup> Yamei Han,<sup>4</sup> Fengguang Ma,<sup>4</sup> Zhimin Hu,<sup>4</sup> Feng-Zhi Xin,<sup>1</sup> Xiao-Lin Liu,<sup>1,5</sup> Tian-Yi Ren,<sup>1</sup> Feifei Zhang,<sup>4</sup> Yaqian Xue,<sup>4</sup> Aoyuan Cui,<sup>4</sup> Zhengshuai Liu,<sup>4</sup> Jinyun Bai,<sup>6</sup> Yuxiao Liu,<sup>4</sup> Genxiang Cai,<sup>4</sup> Weitong Su,<sup>4</sup> Xiaozhen Dai,<sup>7</sup> Feng Shen,<sup>1</sup> Qin Pan,<sup>1</sup> Yu Li,<sup>4</sup> and Jian-Gao Fan<sup>1,8</sup>

<sup>1</sup>Center for Fatty Liver, Department of Gastroenterology, Xinhua Hospital Affiliated to Shanghai Jiao Tong University School of Medicine, Shanghai, China; <sup>2</sup>Department of Hepatology, Qilu Hospital of Shandong University, Jinan, China; <sup>3</sup>Department of Gastroenterology and Hepatology, Zhongshan Hospital, Fudan University, Shanghai, China; <sup>4</sup>CAS Key Laboratory of Nutrition, Metabolism and Food Safety, Shanghai Institute of Nutrition and Health, University of the Chinese Academy of Sciences, Chinese Academy of Sciences, Shanghai, China; <sup>5</sup>Department of Gastroenterology, The First Affiliated Hospital of Soochow University, Suzhou, Jiangsu, China; <sup>6</sup>Department of Endocrinology and Metabolism, Zhongshan Hospital, Fudan University, Shanghai, China; <sup>7</sup>School of Bioscience and Technology, Chengdu Medical College, Chengdu, China; and <sup>8</sup>Shanghai Key Lab of Pediatric Gastroenterology and Nutrition, Shanghai, China;



## SUMMARY

NaB mediates the crosstalk between the gut and liver in regulating metabolism, regulates hepatic lipogenesis, and maintains lipid homeostasis via LKB1-AMPK-Insig signaling pathway. Therapeutic approaches, such as LKB1 and Insig activators in hepatocytes, may have potential for the treatment of NAFLD.

**BACKGROUND AND AIMS:** Butyric acid is an intestinal microbiota-produced short-chain fatty acid, which exerts

salutary effects on alleviating nonalcoholic fatty liver disease (NAFLD). However, the underlying mechanism of butyrate on regulating hepatic lipid metabolism is largely unexplored.

**METHODS:** A mouse model of NAFLD was induced with high-fat diet feeding, and sodium butyrate (NaB) intervention was initiated at the eighth week and lasted for 8 weeks. Hepatic steatosis was evaluated and metabolic pathways concerning lipid homeostasis were analyzed.

**RESULTS:** Here, we report that administration of NaB by gavage once daily for 8 weeks causes an augmentation of insulin-induced gene (Insig) activity and inhibition of lipogenic

gene in mice fed with high-fat diet. Mechanistically, NaB is sufficient to enhance the interaction between Insig and its upstream kinase AMP-activated protein kinase (AMPK). The stimulatory effects of NaB on Insig-1 activity are abolished in AMPK $\alpha$ 1/ $\alpha$ 2 double knockout (AMPK $-/-$ ) mouse primary hepatocytes. Moreover, AMPK activation by NaB is mediated by LKB1, as evidenced by the observations showing NaB-mediated induction of phosphorylation of AMPK, and its downstream target acetyl-CoA carboxylase is diminished in LKB1 $-/-$  mouse embryonic fibroblasts.

**CONCLUSIONS:** These studies indicate that NaB serves as a negative regulator of hepatic lipogenesis in NAFLD and that NaB attenuates hepatic steatosis and improves lipid profile and liver function largely through the activation of LKB1-AMPK-Insig signaling pathway. Therefore, NaB has therapeutic potential for treating NAFLD and related metabolic diseases. (*Cell Mol Gastroenterol Hepatol* 2021;12:857-871; <https://doi.org/10.1016/j.jcmgh.2021.05.006>)

**Keywords:** Sodium Butyrate; Insulin-Induced Gene; LKB1; Hepatic Lipogenesis; NAFLD.

**H**epatic steatosis is a major characteristic of nonalcoholic fatty liver disease (NAFLD), which has emerged as a leading cause of chronic liver diseases and a great threaten to the public health worldwide.<sup>1,2</sup> The disruption of lipid metabolism is a pathological basis and driven factor in the progression of NAFLD. Recent studies have highlighted the contribution of irritated de novo lipogenesis under insulin-resistant condition in the pathogenesis of NAFLD.<sup>3,4</sup> Inhibition of lipogenesis has been shown to effectively reduce hepatic insulin resistance and reverse NAFLD,<sup>5,6</sup> which suggests that hepatic de novo lipogenesis is a crucial target to develop novel strategies for treating NAFLD.

Insulin-induced gene (Insig) acts as a potent inhibitor for the cleavage and maturation of the key lipogenic transcription factor SREBP, and plays an important role in the negative feedback regulation of SREBP and hepatic lipogenesis. Insig-1 and Insig-2 are 2 isoforms of Insig which functions to inhibit SREBP activity via the retention of the SCAP/SREBP complex in the endoplasmic reticulum membrane. Overexpression of hepatic Insig-1 has been shown to inhibit SREBP processing and reduce insulin-stimulated lipogenesis, suggesting Insig is a negative regulator of de novo lipogenesis.<sup>7</sup> Adenosine monophosphate (AMP)-activated protein kinase (AMPK) is a key modulator to regulate intracellular metabolism based on nutrient availability and has been demonstrated to directly target and inhibit the activity of SREBP-1c, thereby suppressing hepatic lipogenesis.<sup>8</sup> Interestingly, AMPK phosphorylation of Insig at Thr222 site is required for the protein stabilization of Insig-1 and inhibition of cleavage and processing of SREBP-1 and lipogenic gene expression in response to metformin or A769662, suggesting that posttranslational regulation of Insig plays essential roles in the regulation of lipid metabolism in the liver.<sup>9</sup> Moreover, liver kinase B1 (LKB1) is the major upstream kinase of AMPK, and the LKB1/AMPK signal

plays important roles in the regulation of gluconeogenesis and glucose homeostasis.<sup>10</sup>

Short-chain fatty acids are produced by intestinal commensal bacteria using dietary indigestible fibers, among which butyric acid is one of the most abundant.<sup>11</sup> Previous studies showed that butyrate can be utilized as an energy source in colonocytes.<sup>12,13</sup> Meanwhile, accumulated evidence has demonstrated that butyrate regulates energy metabolism and plays a protective role in the metabolic disorders over the past decade.<sup>14</sup> However, the mechanisms underlying the regulatory role of butyrate have been shown to be multiple and varied under different conditions. Owing to the fact that butyrate is produced and enriched in the intestinal lumen, it has been believed that butyrate exerts local effects on the enteroendocrine L cells and stimulates the production of gut hormones such as peptide YY (PYY) and glucagon-like peptide 1 (GLP-1) to regulate the satiety and energy intake.<sup>14,15</sup> Furthermore, butyrate has been discovered to be able to influence the development, differentiation, and activation of immune cells both in the gut and peripheral tissues, and ameliorates the metabolic inflammation that augments the insulin resistant and metabolic dysfunction.<sup>16-18</sup> Moreover, our previous study found that sodium butyrate (NaB) has an impact on the structure of gut microbiota increasing the abundance of probiotics, strengthening the intestinal barrier and decreasing the gut-derived endotoxemia, leading to the improvement of high-fat diet (HFD)-induced steatohepatitis in a mouse model.<sup>19</sup> These evidence suggest that NaB has systemic effects and protects against metabolic disorders via multiple mechanisms. However, whether the liver is a target tissue of butyrate and how the hepatocytes sense butyrate to facilitate its interaction with the regulation network of energy metabolism are largely unexplored.

We have recently reported that NaB increases hepatic expression of GLP-1 receptor via inhibiting HDAC2 (histone deacetylase 2), which sensitizes the effects of NaB on inhibiting lipid synthesis and augmentation of fatty acid oxidation in hepatocytes and leads to a reduction of hepatic steatosis.<sup>20</sup> In this study, we provide insights into the mechanism by which NaB regulates the lipid metabolism in a hepatocyte-autonomous manner. These in vivo and in vitro studies demonstrate that (1) pharmacological administration of NaB improves hepatic steatosis in diet-induced mice, (2) the stimulatory effects of NaB on Insig-1 activity are dependent on AMPK, (3) LKB1 is required for

\*Authors share co-first authorship

**Abbreviations used in this paper:** ACC, acetyl-CoA carboxylase; AMP, adenosine monophosphate; AMPK, AMP-activated protein kinase; ATP, adenosine triphosphate; GLP-1, glucagon-like peptide 1; GST, glutathione S-transferase; HFD, high-fat diet; Insig, insulin-induced gene; LKB1, liver kinase B1; NaB, sodium butyrate; NAFLD, nonalcoholic fatty liver disease; PYY, peptide YY.



Most current article

© 2021 The Authors. Published by Elsevier Inc. on behalf of the AGA Institute. This is an open access article under the CC BY-NC-ND license (<http://creativecommons.org/licenses/by-nc-nd/4.0/>).

2352-345X

<https://doi.org/10.1016/j.jcmgh.2021.05.006>

the activation of AMPK in response to NaB treatment, and (4) NaB inhibits hepatic lipogenesis via LKB1-AMPK-Insig signaling pathway.

## Results

### *Administration of NaB Attenuates Hepatic Steatosis in Mice Fed With HFD*

To study the regulatory role of NaB in NAFLD, administration of 200 mg/kg NaB in mice by gavage was performed, which has been used in other mouse models of atherosclerosis, Parkinson's disease, and so on.<sup>21–24</sup> To assess the efficacy of exogenous NaB administration and the alteration of butyric acid concentration in portal circulation, blood was collected from the portal vein in mice treated without or with 200 mg/kg NaB and liquid chromatography tandem mass spectrometry analysis was performed to measure portal levels of butyric acid. We found that the physiological level of butyric acid in the portal vein in mice are around 2  $\mu\text{g/mL}$  ( $2.142 \pm 2.438 \mu\text{g/mL}$ ,  $n = 6$ ), which is comparable to the levels of 3.3  $\mu\text{g/mL}$  in portal vein of health humans,<sup>25</sup> whereas NaB treatment causes a 4-fold induction of butyric acid ( $8.245 \pm 3.554 \mu\text{g/mL}$ ,  $n = 6$ ). These results suggest that the administration of 200 mg/kg NaB is sufficient to cause the induction of portal butyric acid concentration. Next, administration of 200 mg/kg NaB by gavage once daily for 8 weeks was initiated in mice fed with chow or HFD at the eighth week and lasted for 8 weeks (Figure 1A). At the end of 16th week, the livers were harvested and the lipid profile was analyzed. As shown in Figure 1B and C, the hepatic levels of triglycerides and cholesterol were greatly induced in mice fed with HFD, and was significantly decreased by NaB treatment. The hematoxylin and eosin staining of liver sections showed both macrovesicular and microvesicular steatosis in mice fed with HFD, which was alleviated in mice treated with NaB (Figure 1D). Furthermore, we evaluated the histological severity of hepatic steatosis using the steatosis score based on the SAF scoring system.<sup>26</sup> The results showed that NaB treatment significantly decreased the steatosis score (Figure 1E). Meanwhile, the oil red O staining also demonstrated the amelioration of lipid accumulation in the livers by NaB treatment (Figure 1D and F). Moreover, we also quantified the serum levels of triglycerides (Figure 1G), total cholesterol (Figure 1H), alanine aminotransferase (Figure 1I), and aspartate aminotransferase (Figure 1J). The serum parameters were all improved with NaB intervention, which was consistent with our previous results.<sup>19</sup> These data demonstrated improvement of both histological and serum alterations by 8-week NaB treatment and suggest a protective role of NaB in HFD-induced hepatic steatosis.

### *Administration of NaB Causes an Augmentation of Insig Activity and Inhibition of Lipogenic Gene Expression in Mice Fed With HFD*

Insig is a pivotal regulator in lipid metabolism. The 2 isoforms Insig-1 and Insig-2 function similarly and Insig-1 is highly expressed in the liver. Thus, we then explore the effect

of NaB treatment on the protein levels of Insig-1 and Insig-2. Interestingly, hepatic protein levels of Insig-1 were reduced in mice fed with HFD and significantly restored in the mice treated with NaB, which was evidenced by immunohistochemistry staining (Figure 2A) and immunoblots (Figure 2B and C). Similarly, protein levels of Insig-2 were restored in the livers of mice receiving 8-week NaB intervention (Figure 2A, B, and D). These results suggest that NaB treatment induces Insig protein level. We then examined the effect of NaB on the protein expression of downstream lipogenic genes. The results showed that the protein levels of SCD1 (Figure 2F and G), FAS (Figure 2F and H), and the nuclear form of SREBP-1 (68 kD) (Figure 2F and I) were all strikingly downregulated in HFD-fed mice treated with NaB. Taken together, these data indicate that NaB treatment is able to inhibit the expression of lipogenic genes through restoring protein levels of Insig in the livers of mice fed with HFD.

### *The Inhibitory Effects of NaB on Lipogenic Gene Expression and Lipid Accumulation Are Mediated by Stimulating Insig in Hepatocytes*

To further examine the regulation of NaB on Insig, we next conducted *in vitro* experiments. HEK293 cells were transfected with plasmid encoding Insig and then treated with NaB.<sup>9</sup> As shown in Figure 3A and B, NaB treatment significantly increases the protein levels of both Insig-1 and Insig-2 in a dose-dependent manner. Therefore, we hypothesized NaB may stimulate the expression of Insig to inhibit *de novo* lipogenesis. To further testify the hypothesis, we investigated the effect of NaB in HepG2 hepatocytes exposed to high glucose plus insulin.<sup>27</sup> As shown in Figure 3C, the protein levels of SCD1 and FAS were significantly induced by treatment with high glucose plus insulin and suppressed by NaB in a dose-dependent manner, which was consistent with the *in vivo* data. Moreover, Oil Red O staining and BODIPY staining were performed to explore the function of NaB in response to glucose and insulin stimulation. As shown in Figure 3D, the lipid droplets were significantly induced by treatment with high glucose plus insulin and reduced with 5 mM and 10 mM NaB treatment in HepG2 cells. Quantification of both triglycerides (Figure 3E) and BODIPY fluorescence intensity (Figure 3F) revealed a potent inhibitory effect of NaB on lipid accumulation. Taken together, *in vitro* results suggest that NaB increases protein levels of Insig and inhibits *de novo* lipogenesis by downregulating lipogenic gene expression.

### *The Effects of NaB on Stimulating Insig-1 Are Dependent on AMPK*

We have recently identified Insig as a novel target of AMPK in the posttranslational regulation of lipogenesis.<sup>9</sup> To determine the role of AMPK in NaB's regulation of Insig, we first investigate the effect of NaB on the activity of AMPK. Strikingly, the phosphorylation of AMPK and its downstream target acetyl-CoA carboxylase (ACC) was increased by NaB treatment in mice fed with HFD compared with vehicle control, which was evidenced by immunohistochemistry staining (Figure 4A) and immunoblots (Figure 4B

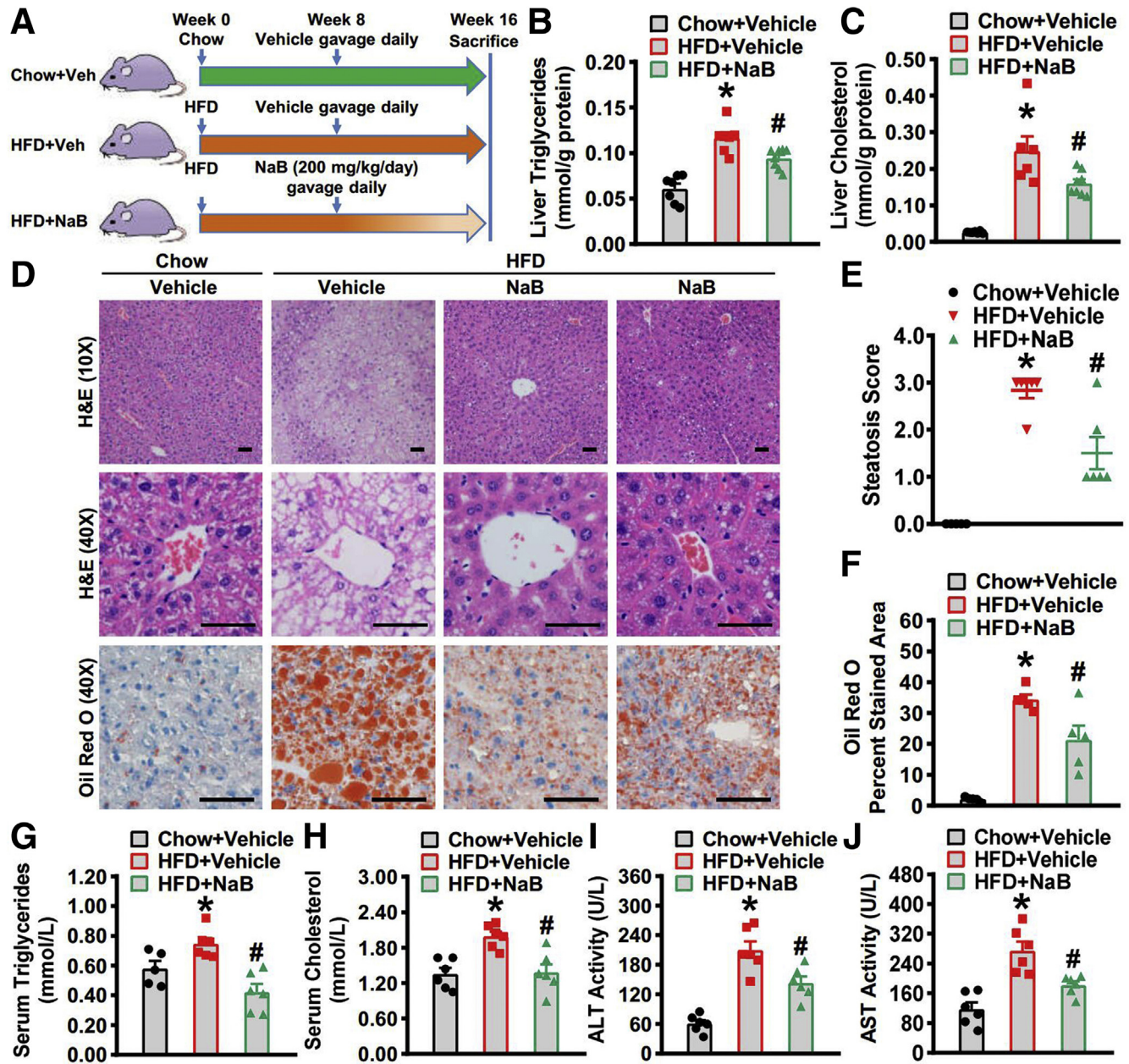


**Figure 1. Beneficial effects of NaB on lowering hepatic steatosis in mice fed with HFD.** Eight-week-old male C57BL/6 mice were fed with a HFD for 8 weeks, and then gavaged with NaB (1 g/kg/d) or vehicle (phosphate-buffered saline) for 8 weeks. Mice were sacrificed at the end of 16th week and livers were harvested. (A) Schematic illustration showing the design of the in vivo experiment. (B) Hepatic triglycerides and (C) cholesterol levels were assessed in mice ( $n = 6-8$ ). (D) Representative hematoxylin and eosin (H&E) and Oil Red O stainings of the liver sections are shown (scale bar = 50  $\mu\text{m}$ ). (E) Steatosis score based on the SAF score algorithm is measured ( $n = 6$ ). (F) Quantification of Oil Red O-stained areas is shown ( $n = 6$ ). Serum levels of (G) triglycerides, (H) cholesterol, (I) alanine aminotransferase, and (J) aspartate aminotransferase are detected ( $n = 5-6$ ). The data are presented as the mean  $\pm$  SEM, unpaired 2-tailed Student's  $t$  test,  $n = 5-8$ . \* $P < .05$  vs mice fed with chow diet; # $P < .05$  vs mice fed with HFD.

and C). These results suggest that the activity of AMPK was significantly restored by NaB intervention under nutrition overload conditions. To further clarify whether AMPK is required in the regulation of Insig by NaB, we isolated primary hepatocytes from AMPK $\alpha 1/\alpha 2$  double knockout (AMPK $^{-/-}$ ) mice, which were infected with adenoviruses overexpressing Insig-1 and followed by NaB treatment. As

shown in Figure 4D, in contrast to AMPK wild-type hepatocytes, the induction of Insig-1 by NaB treatment was potentially abolished in AMPK $^{-/-}$  hepatocytes. Notably, a mild induction of Insig-1 by NaB treatment suggests the existence of an AMPK-independent mechanism, which requires further investigation. Taken together, NaB is able to activate AMPK and regulates Insig in an AMPK-dependent manner.

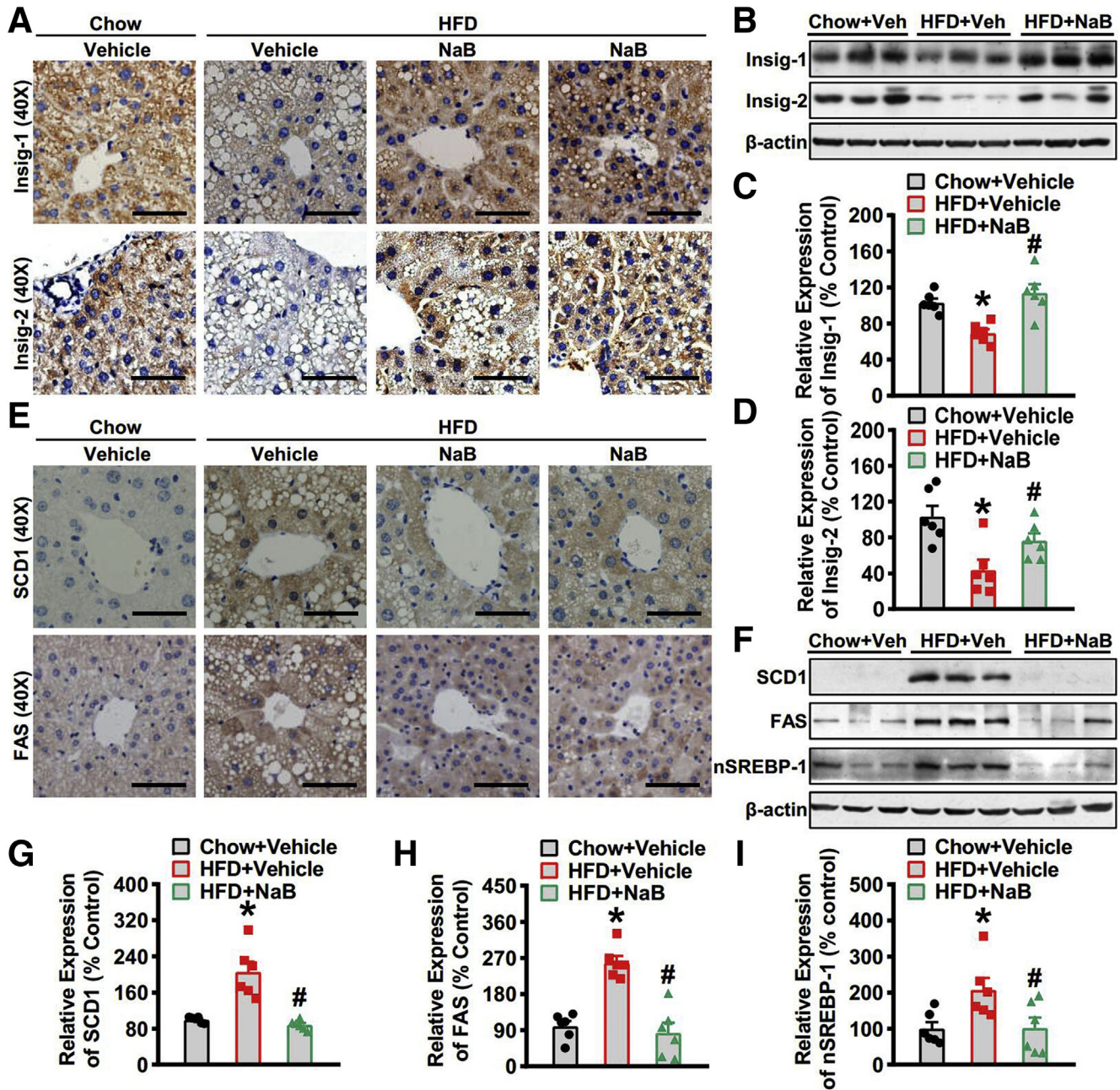


**Figure 2.** Administration of NaB stimulates the activity of Insig to inhibit lipogenic gene expression in mice fed with HFD. (A–C) The protein levels of Insig-1 and Insig-2 are increased in the liver of mice treated with NaB. (A) Representative immunohistochemical staining of the liver sections with Insig-1 and Insig-2 antibodies (scale bar = 50  $\mu$ m). (B) Immunoblots were performed, and the band intensity of (C) Insig-1 and (D) Insig-2 was quantified by densitometry (n = 6). (E–I) The protein levels of lipogenic genes are decreased in the liver of mice treated with NaB. (E) Representative immunohistochemical staining of the liver sections with SCD1 and FAS antibodies (scale bar = 50  $\mu$ m). (F) Immunoblots were performed, and the band intensity of (G) SCD1, (H) FAS, and (I) nuclear SREBP-1 was quantified by densitometry (n = 6). The data are presented as the mean  $\pm$  SEM, unpaired 2-tailed Student's *t* test, n = 6. \**P* < .05 vs mice fed with chow diet; #*P* < .05 vs mice fed with HFD.

### The Interaction Between Insig and Its Upstream Kinase AMPK Is Increased by NaB Treatment

Our previous findings have revealed a novel mechanism in which AMPK directly interacts with and mediates phosphorylation of Insig at Thr222, resulting in the reduction of ubiquitination and degradation of Insig.<sup>9</sup> Given that we have shown NaB is able to increase protein levels of Insig and

restore the activity of AMPK under nutrition overload conditions, we further explored the effect of NaB on the interaction between Insig and AMPK. HEK293 cells stably overexpressing Insig were transfected with AMPK $\alpha$  vectors and treated with NaB. The co-immunoprecipitation assay showed that NaB treatment significantly enhanced the association of AMPK $\alpha$ 2 with both Insig-1 (Figure 5A) and

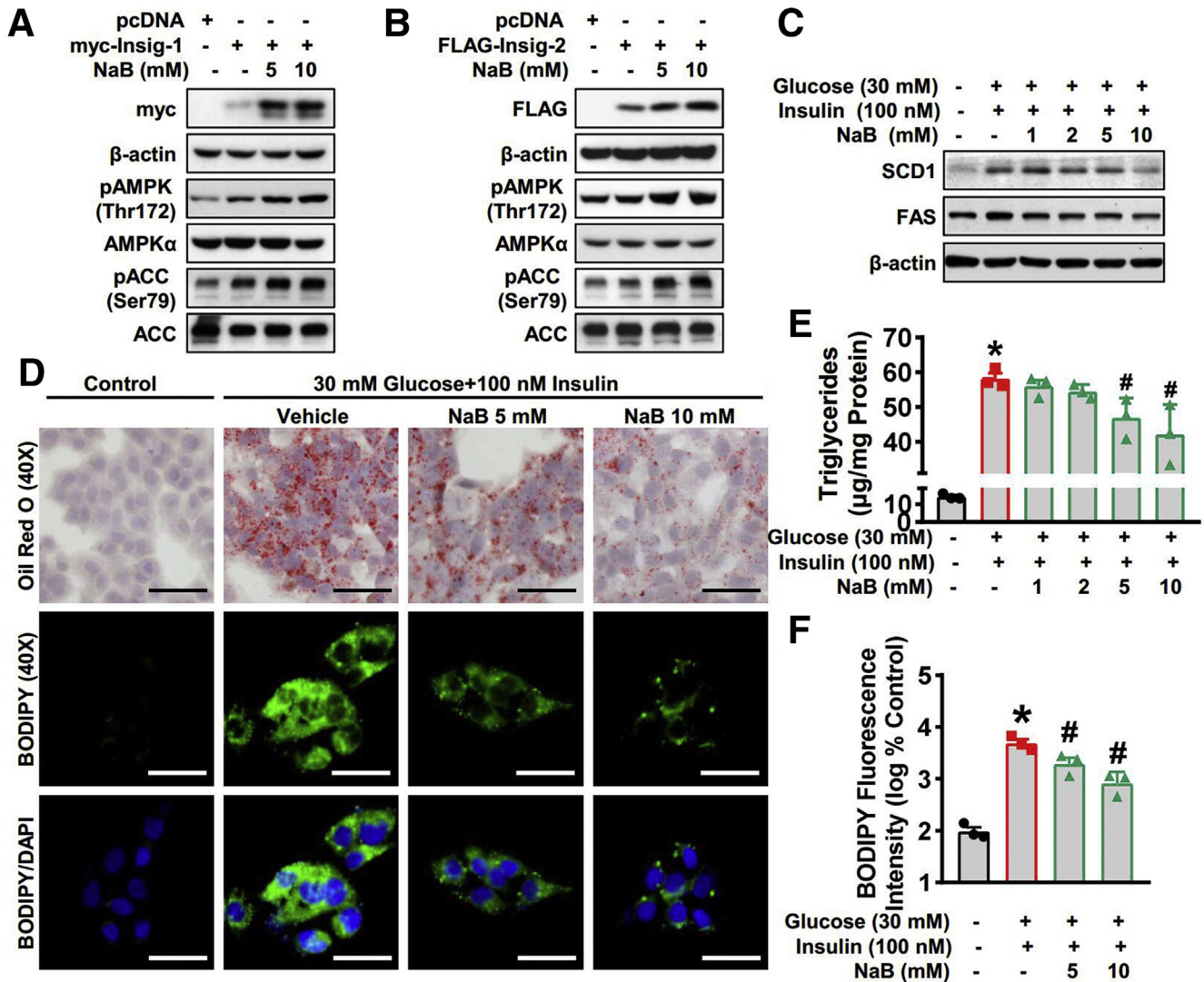


**Figure 3. NaB inhibits lipogenic gene expression and lipid accumulation by enhancing Insig activity in hepatocytes.** (A, B) NaB treatment increases protein levels of Insig. HEK293 cells were transfected with pcDNA, Myc-tagged Insig-1, or FLAG-tagged Insig-2 for 24 hours, followed by treatment with 5 mM or 10 mM NaB as indicated. Immunoblots were performed. (C–F) NaB treatment decreases protein levels of lipogenic enzymes and alleviates lipid accumulation in human HepG2 cells exposed to high glucose plus insulin. HepG2 cells were fasted for 24 hours, followed by 30 mM glucose and 100 nM insulin treatment, together with NaB (1–10 mM) or vehicle (phosphate-buffered saline) treatment. (C) Immunoblots show that NaB treatment decreases protein levels of SCD-1 and FAS in a dose-dependent manner. (D–F) Triglycerides accumulation is attenuated with 5 mM and 10 mM NaB treatment. (D) Representative oil red O staining (scale bar = 50 µm) and (E) the quantification of triglycerides are shown (n = 3). (D) Representative BODIPY staining (scale bar = 50 µm) and (F) the quantification are shown (n = 3). The data are presented as the mean ± SEM, unpaired 2-tailed Student's *t* test, n = 3. \**P* < .05 vs vehicle; #*P* < .05 vs treatment with high glucose plus insulin.

Insig-2 (Figure 5B) in a dose-dependent manner. Similarly, the interaction between AMPKα1 and Insig was also strengthened by NaB treatment in a dose-dependent manner (Figure 5C and D). Given that NaB enhances protein levels of Insig, we cannot exclude the possibility that the increased interaction between Insig and AMPK in response to NaB treatment is due to elevated Insig protein. Taken together, these data imply that NaB likely enhances the interaction between AMPK and Insig, facilitating the Insig phosphorylation by AMPK leading to the decline of

ubiquitination-mediated degradation, which contributes to the induction of Insig by NaB treatment.

#### *LKB1 Phosphorylation and Intracellular Energy Levels Mediate the Stimulatory Effects of NaB on AMPK Activity*

Now that we have discovered that AMPK activation mediates the regulation of Insig by NaB, we sought to determine the upstream mechanisms underlying the

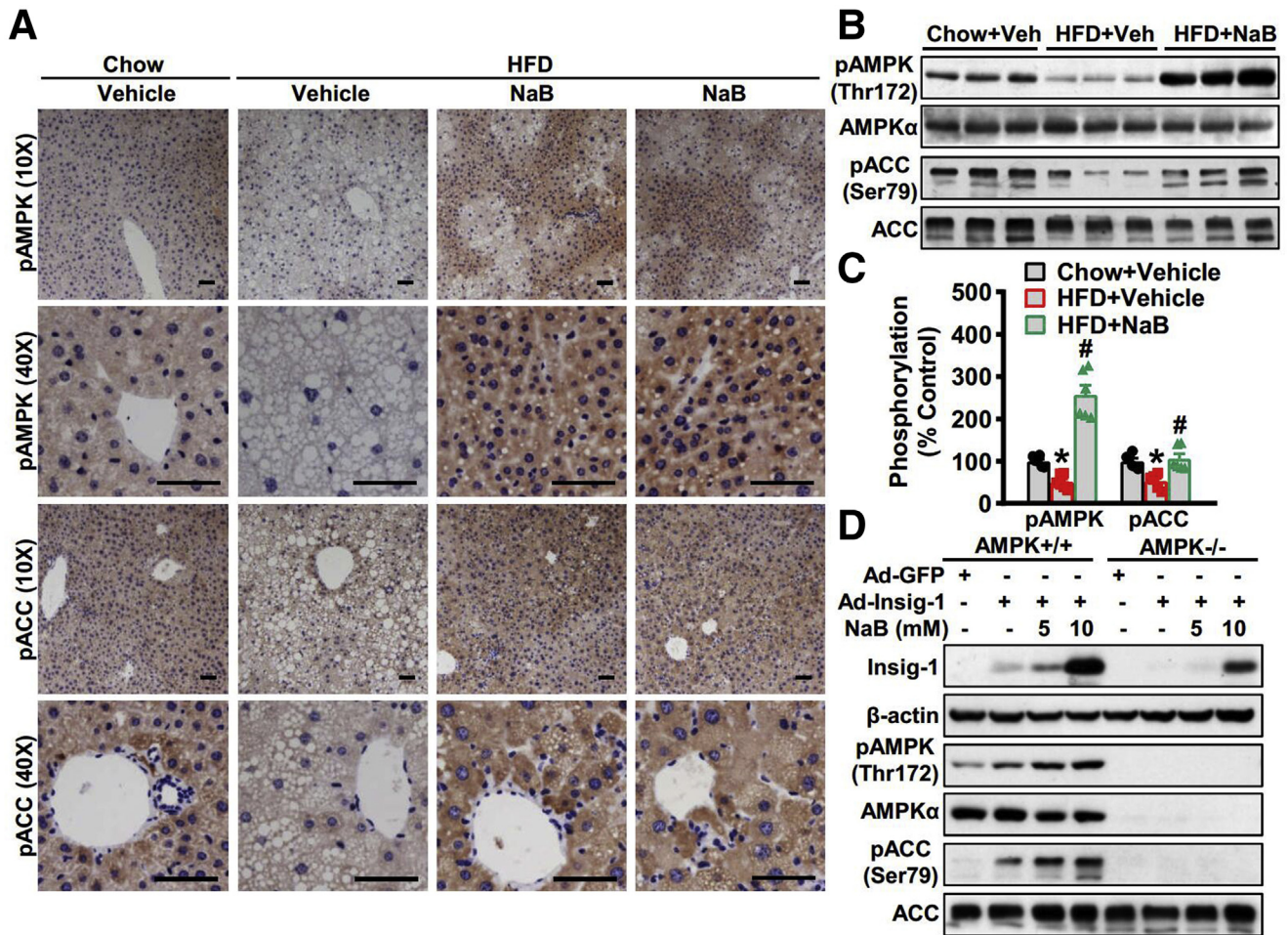


**Figure 4. AMPK is required for Insig-1 induction in response to NaB treatment.** (A–C) NaB increases the expression levels of phosphorylated AMPK in mice fed with HFD. (A) Representative immunohistochemical staining of the liver sections with phosphorylated AMPK (pAMPK) and phosphorylated ACC (pACC) antibodies (scale bar = 50  $\mu$ m). (B) Immunoblots were performed, and (C) the band intensity of pAMPK and pACC was quantified by densitometry ( $n = 6$ ). (D) AMPK is required for Insig-1 induction in response to NaB treatment. AMPK<sup>+/+</sup> or AMPK $\alpha$ 1/ $\alpha$ 2 double knockout (AMPK<sup>-/-</sup>) mouse primary hepatocytes were infected with adenoviruses encoding Insig-1 (Ad-Insig-1) or green fluorescent protein (GFP) for 24 hours, followed by treatment with 5 mM or 10 mM NaB for 24 hours. The data are presented as the mean  $\pm$  SEM, unpaired 2-tailed Student's  $t$  test,  $n = 6$ . \* $P < .05$  vs mice fed with chow diet; # $P < .05$  vs mice fed with HFD.

activation of AMPK by NaB treatment. LKB1 is a major upstream kinase of AMPK.<sup>28</sup> Thus, we explored the effect of NaB on the LKB1 activity in HepG2 cells. As shown in Figure 6A and C, protein levels of phosphorylated LKB1 were greatly induced by treatment with 5 mM and 10 mM NaB, which was consistent with the change of AMPK phosphorylation (Figure 6B and D). These data indicate that the kinase activity of LKB1 is induced by NaB treatment, leading to the activation of AMPK. Next, we determined whether LKB1 is required for NaB's activation of AMPK. As shown in Figure 6E, the phosphorylation of AMPK was greatly suppressed by treatment with high glucose plus insulin and restored by NaB treatment in a dose-dependent manner in LKB1 wild-type MEF cells, whereas AMPK was failed to be activated by NaB treatment under LKB1 deficient conditions. These results suggest that NaB induces the kinase activity of LKB1 and activates AMPK in an LKB1-dependent manner.

AMPK functions as a sensor of the intracellular energy state, whose gamma subunit can sense the alteration of AMP and adenosine triphosphate (ATP) to adjust its kinase activity.<sup>29</sup> Therefore, we then investigate the effect of NaB on the levels of AMP and ATP. Human HepG2 cells were treated with glucose and insulin, together with vehicle or NaB in different doses, and subjected to separate AMP and ATP quantification. As shown in Figure 6F, the intracellular levels of both AMP and ATP were induced when treated with high glucose plus insulin, which was decreased by NaB treatment in a dose-dependent manner. Notably, the extent of decline in ATP was superior to AMP in NaB-treated HepG2 cells, leading to the dramatic elevation of AMP-to-ATP ratio (Figure 6G). These data indicate that NaB may modulate the AMP-to-ATP ratio to facilitate AMPK activation. Furthermore, to understand the possible mechanisms underlying the prominent reduction of ATP in NaB-treated HepG2 cells, we examined the effect of NaB on

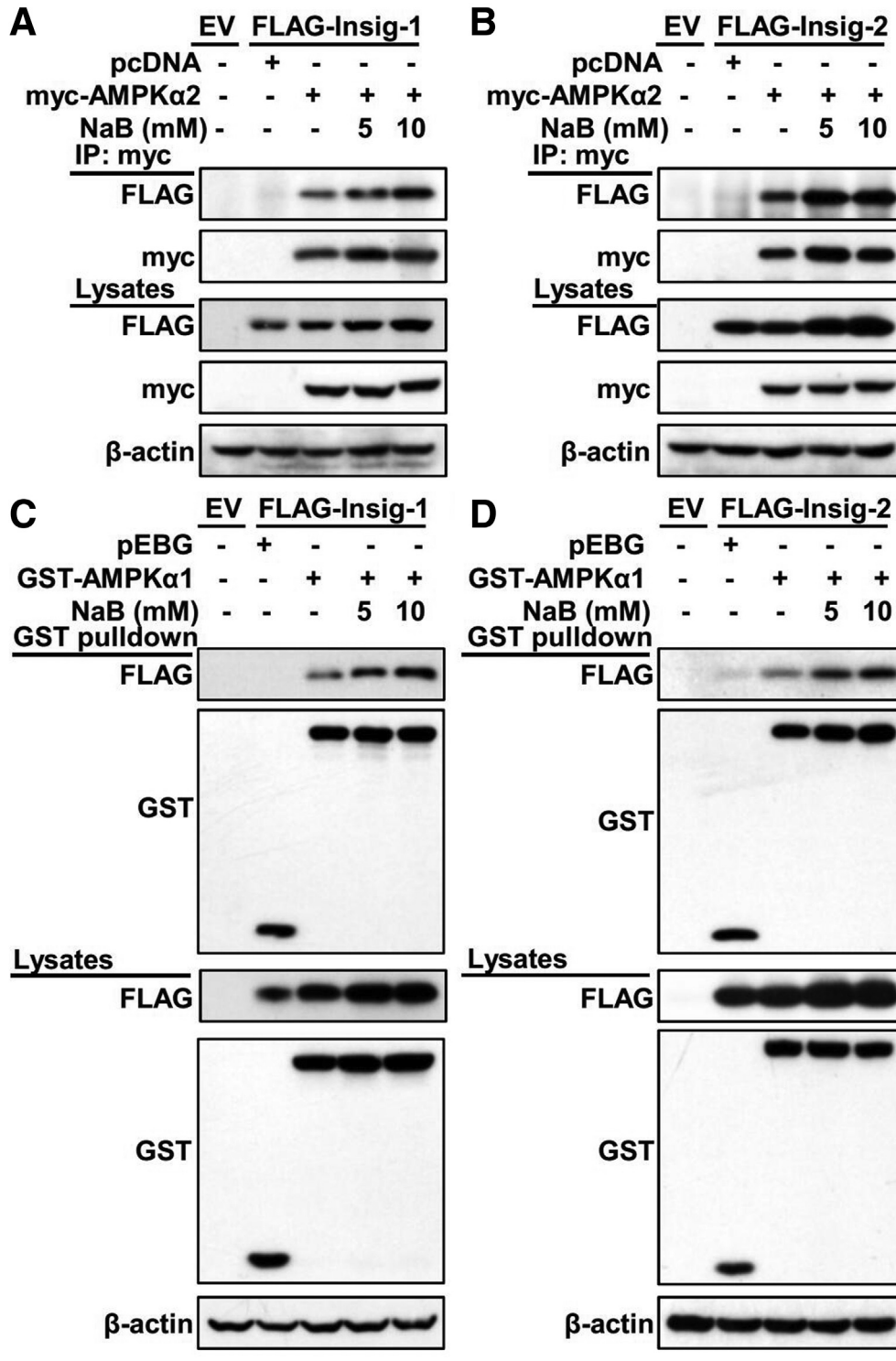


**Figure 5. Administration of NaB enhances the interaction between Insig and its upstream kinase AMPK.** (A, B) NaB enhances the association of AMPK $\alpha$ 2 subunit with Insig in a dose-dependent manner. FLAG-tagged (A) Insig-1 or (B) Insig-2 was co-transfected with Myc-tagged AMPK $\alpha$ 2 in HEK293 cells for 24 hours, followed by treatment with 5 mM or 10 mM NaB for 24 hours. The cell lysates were incubated with Myc antibodies and purified with protein A/G-Sepharose beads. The precipitates and lysates were individually immunoblotted with indicated antibodies. (C, D) NaB enhances the association of AMPK $\alpha$ 1 subunit with Insig in a dose-dependent manner. FLAG-tagged (C) Insig-1 or (D) Insig-2 was co-transfected with GST-tagged AMPK $\alpha$ 1 in HEK293 cells for 24 hours, followed by treatment with 5 mM or 10 mM NaB for 24 hours. The cell lysates were then purified with GST Sepharose beads. The precipitates and lysates were immunoblotted with antibodies against FLAG or GST. EV, empty vector; IP, immunoprecipitation.

the expression of mitochondrial respiratory chain complex that governs the process of oxidative phosphorylation, which is a major source of ATP production. Unlike the inhibitory effect of other AMPK agonists such as metformin and berberine on mitochondrial respiratory chain complex I,<sup>30,31</sup> we found that NaB had minimal effect on protein levels of mitochondrial respiratory chain complex in both

human HepaG2 cells (Figure 6H) and mouse primary hepatocytes (Figure 6I), suggesting that NaB may affect the ATP-consuming process, rather than sabotage the ATP-producing process. Taken together, our results suggest that LKB1 is activated and AMP-to-ATP ratio is elevated with NaB treatment, contributing to the activation of AMPK by NaB.



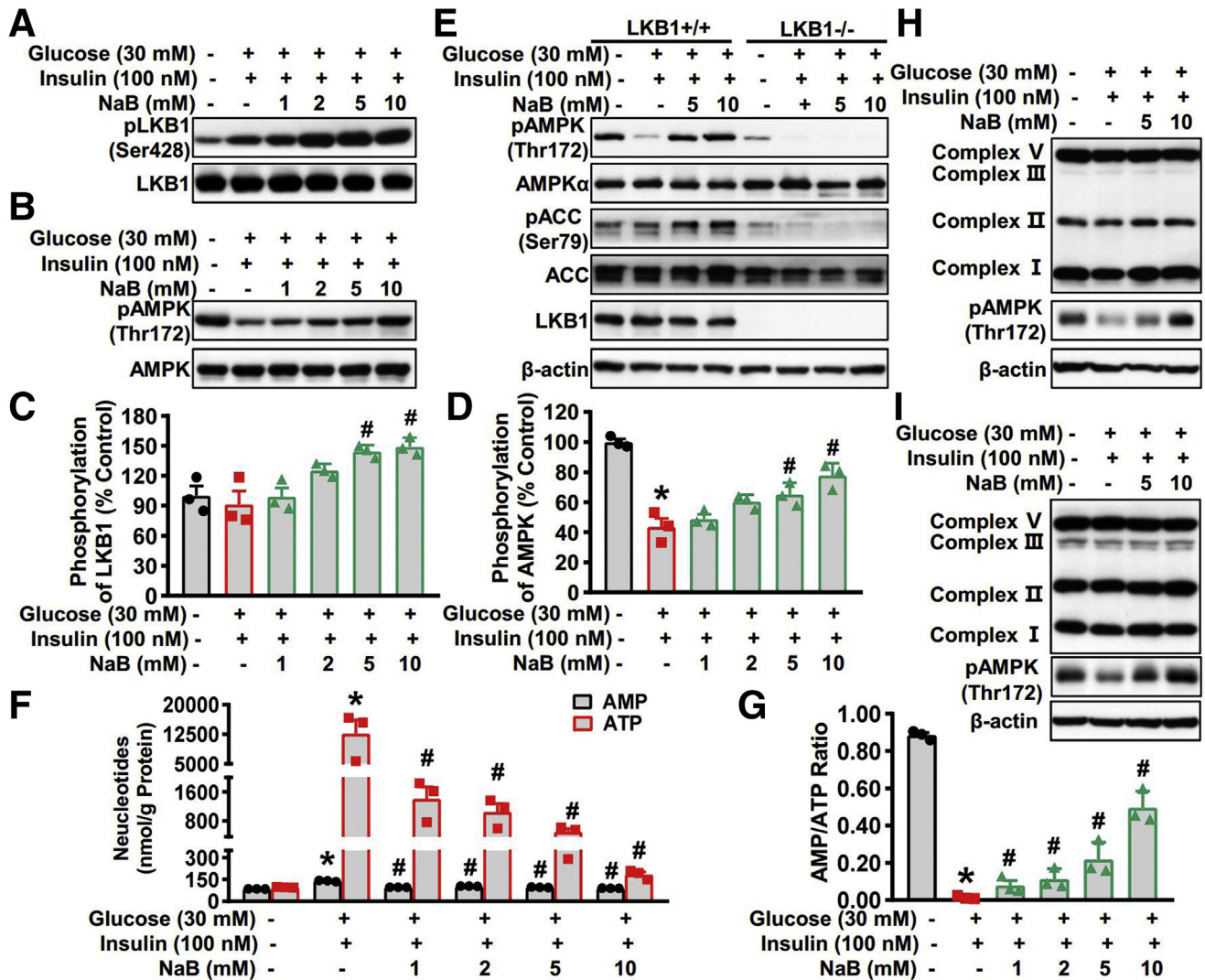


**Figure 6.** The stimulatory effects of NaB on AMPK activity are mediated by LKB1 phosphorylation and intracellular energy levels. (A–D) NaB increases levels of phosphorylated LKB1 and phosphorylated AMPK in a dose-dependent manner in HepG2 cells. HepG2 cells were fasted for 24 hours, followed by 30 mM glucose and 100 nM insulin treatment, together with NaB (1–10 mM) or vehicle (phosphate-buffered saline) treatment. (A) Immunoblots show that NaB treatment increases phosphorylation of LKB1 in a dose-dependent manner. (C) The band intensity of phosphorylated LKB1 was quantified by densitometry ( $n = 3$ ). (B) Immunoblots show that NaB treatment increases phosphorylation of AMPK in a dose-dependent manner. (D) The band intensity of phosphorylated AMPK (pAMPK) was quantified by densitometry ( $n = 3$ ). (E) LKB1 is required for AMPK activation in response to NaB treatment. LKB1<sup>-/-</sup> mouse embryonic fibroblasts were fasted for 24 hours, followed by 30 mM glucose and 100 nM insulin treatment, together with NaB (5 mM and 10 mM) or vehicle (phosphate-buffered saline) treatment. (F, G) NaB treatment regulates the levels of AMP and ATP and increases AMP-to-ATP ratio in HepG2 cells exposed to high glucose plus insulin. HepG2 cells were fasted for 24 hours, followed by 30 mM glucose and 100 nM insulin treatment, together with different doses of NaB (1–10 mM) or vehicle (phosphate-buffered saline) treatment, and then the lysates were subjected to AMP and ATP detection. (F) The levels of AMP and ATP were quantified and (G) the AMP-to-ATP ratio were calculated. (H, I) Protein levels of mitochondrial electron transport chain complex are not altered by NaB treatment. Immunoblots were performed in (H) human HepG2 cells and (I) mouse primary hepatocytes. The data are presented as the mean  $\pm$  SEM, unpaired 2-tailed Student's  $t$  test,  $n = 3$ . \* $P < .05$  vs vehicle; # $P < .05$  vs treatment with high glucose plus insulin. pACC, phosphorylated acetyl-CoA carboxylase.

## Discussion

The metabolic benefits of NaB have been identified in several different metabolic disorders, including type 2 diabetes, cardiovascular disease, and NAFLD.<sup>19,32,33</sup> However, the underlying mechanisms are not fully illuminated. Here, we demonstrate that administration of NaB

stimulates Insig activity and represses de novo lipogenesis via enhancing the phosphorylation of AMPK. Importantly, the tumor suppressor LKB1 is required for NaB-induced phosphorylation and activation of AMPK. The LKB1-AMPK-Insig axis may represent a novel mechanism by

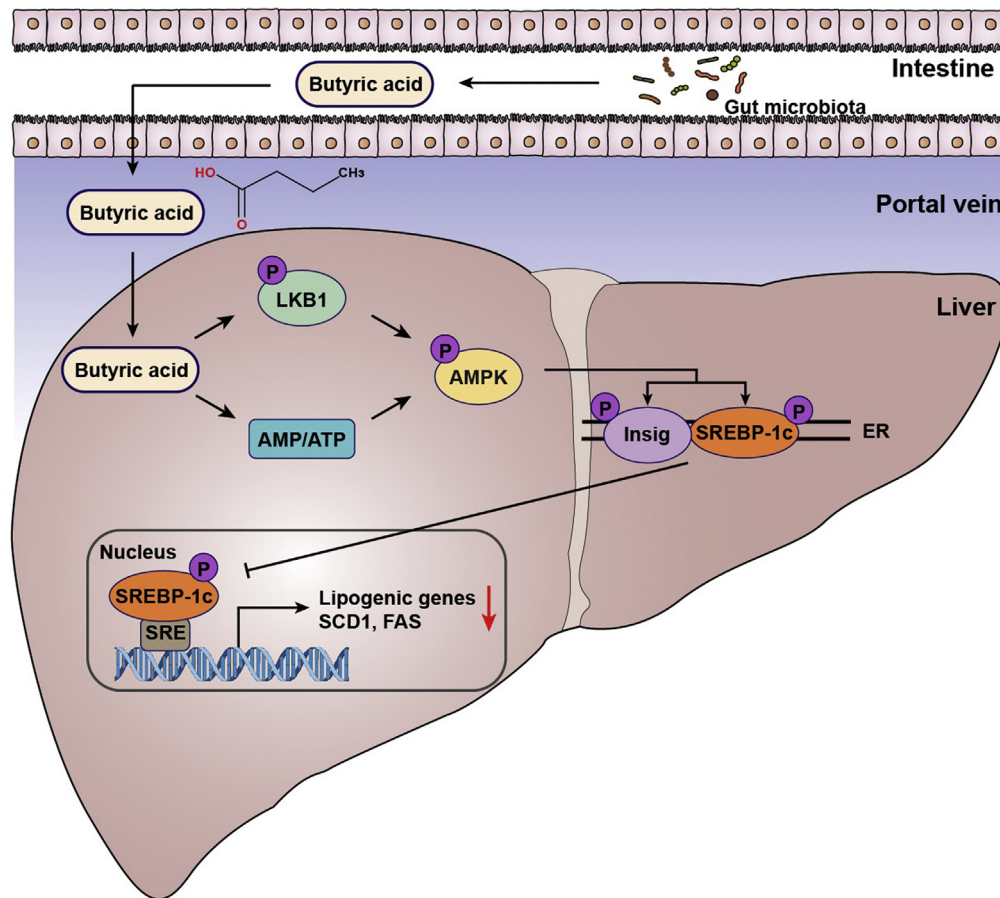


**Figure 7. The proposed model for butyric acid-mediated inhibition of lipogenesis via LKB1-AMPK-Insig signaling pathway.** Gut-derived metabolite butyric acid exerts beneficial effects on hepatocytes, enhancing LKB1 phosphorylation and elevating AMP-to-ATP ratio, which facilitates AMPK activation. Subsequently, interaction between AMPK and Insig is strengthened by butyric acid, resulting in phosphorylation of Insig at Thr222 and decline of proteasome-mediated degradation. The increased Insig restrains the processing and translocation of SREBP-1c and suppresses its transcriptional activity. The activation of AMPK by butyric acid also facilitates SREBP-1c phosphorylation at Ser372 and suppresses its proteolytic cleavage. These mechanisms by which butyric acid inhibits *de novo* lipogenesis in hepatocytes provide therapeutic potential for hepatic steatosis management. ER, endoplasmic reticulum.

which NaB attenuates hepatic steatosis under nutrition overload conditions (Figure 7).

### *The Liver Is a Target Tissue of NaB Actions to Improve Lipid Metabolism*

The effect of butyric acid has been investigated in the metabolic disorders for a long time. Most studies have focused on its regulatory role in the intestinal lumen in which butyric acid exists at the highest concentration. Protective effects of butyrate on the intestinal barrier and functions of immune cells have been identified.<sup>19,34</sup> Apart from the local effects in the intestines, the systemic effects of butyrate have also been reported, many of which are mediated by the gut hormones such as GLP-1 and PYY secreted by the enteroendocrine L cells. Moreover, butyrate has been found to act on the gut-brain neural circuit to improve energy metabolism, leading to a reduction of energy intake and induction of fat oxidation via enhancing brown adipose tissue activity.<sup>35</sup>

Our recent findings demonstrate that administration of NaB sensitizes GLP-1's effects on inhibiting lipid synthesis and augmentation of fatty acid oxidation in hepatocytes and leads to a reduction of hepatic steatosis, suggesting that hepatocytes are sufficient to sense the gut-derived signaling pathway in response to NaB. However, whether NaB stimulates the signaling pathway in hepatocytes to regulate metabolic homeostasis is largely unknown. The present study provides the evidences showing that liver is a target tissue of NaB actions to improve lipid metabolism. First, pharmacological administration of NaB causes a significant reduction of lipogenic gene expression and attenuation of hepatic steatosis in mice fed with HFD. Second, NaB is sufficient to inhibit lipogenesis and triglycerides accumulation in HepG2 hepatocytes exposed to high glucose plus insulin, suggesting that NaB improves hepatic lipid metabolism in a hepatocyte-autonomous manner. Moreover, the activity of the central metabolic sensor AMPK is potently increased in response to NaB treatment in the liver of mice fed with high

fat diet, human HepG2 cells, and primary mouse hepatocytes, further supporting the notion that NaB exerts beneficial actions in the liver to control hepatic lipid homeostasis. Together, these results highlight the importance of NaB on cellular metabolism, and shed light on the novel finding that NaB couples the key metabolic sensor and metabolic signaling pathways to regulate hepatic lipid metabolism.

### *Insig Activation Mediates the Effects of NaB on Alleviating Hepatic Steatosis*

One of the most important findings of the present study is the identification of Insig as an important target in mediating beneficial effects of NaB on lipid metabolism. Insig is known to play pivotal roles in inhibiting de novo lipogenesis via interacting with the SCAP-SREBP complex. This study demonstrates that NaB increases Insig activity via stimulating phosphorylation of AMPK and leads to enhanced interaction between AMPK and Insig and attenuated hepatic steatosis, which are consistent with the recent findings showing that Thr222 phosphorylation of Insig-1 by AMPK is required for the protein stabilization of Insig-1 and inhibition of cleavage and processing of SREBP-1 and lipogenic gene expression.<sup>9</sup> Moreover, phosphorylation of Insig-1 at Ser207 and Insig-2 at Ser151 by PCK1 (phosphoenolpyruvate carboxykinase 1) disrupts the interaction between Insig and SCAP, which leads to the translocation of the SCAP-SREBP complex to the Golgi apparatus and activation of SREBP and its downstream lipogenic gene expression.<sup>36</sup> These studies suggest that posttranslational modification of Insig plays a critical role in the regulation of the proteolytic cleavage and maturation of SREBP and lipogenesis in the liver. Intriguingly, recent studies have reported beneficial effects of activating Insig activity on improving lipid metabolism and attenuating hepatic steatosis. It was reported that R- $\alpha$ -lipoic acid induces expression of Insig-1 and Insig-2a and leads to a reduction of triglycerides accumulation in the liver of diabetic rat and attenuation of hypertriglyceridemia.<sup>37</sup> Moreover, supplementation of omega-3 polyunsaturated fatty acids increases hepatic expression of Insig-1 and improves lipid profile and other metabolic parameters in stress-induced metabolic disorders in rats.<sup>38</sup> Together, these studies indicate that Insig activation plays an important role in mediating NaB's lipid-lowering effects in hepatocytes, and that pharmacological manipulating Insig activity may provide therapeutic strategies for treating lipid dysregulation and related metabolic diseases.

### *The Stimulatory Effects of NaB on AMPK Phosphorylation and Its Downstream Signaling Are Regulated in an LKB1-Dependent Manner in Hepatocytes*

The present study demonstrates that phosphorylation of AMPK and ACC are not increased in response to NaB treatment in LKB1<sup>-/-</sup> mouse embryonic fibroblasts, strongly supporting the notion that AMPK activation by NaB is mediated by LKB1. Given that LKB1 is necessary for

AMPK's salutary effects on inhibiting lipogenic gene expression and lowering circulating glucose levels,<sup>10</sup> LKB1 appears to be an attractive candidate in mediating NaB/AMPK signaling in regulating hepatic lipid metabolism. Although the precise mechanism by which NaB activates LKB1 remains unclear, it is possible that NaB regulates Ser428 phosphorylation of LKB1 via recruiting other protein kinases. Intriguingly, the findings that NaB stimulates AMP-to-ATP ratio to enhance phosphorylation of AMPK indicate that, in addition to LKB1 signaling, AMPK activity may be potentiated in response to NaB treatment. Previous studies have shown that metabolic functions of short-chain fatty acids are mediated by a G protein-coupled receptor-dependent manner, such as GPR43, GPR41.<sup>11</sup> The current study support the notion that NaB regulates lipid metabolism in a G protein-coupled receptor-independent manner, which is consistent with the findings showing NaB's GLP-1 sensitizing effects on inhibiting lipid synthesis and augmentation of fatty acid oxidation in hepatocytes.<sup>20</sup> Together, this study reported an unknown regulator for LKB1/AMPK signaling, which plays an essential role in the regulation of hepatic lipid metabolism.

In conclusion, this study identified a novel mechanism that butyric acid, one of the most abundant short-chain fatty acids produced by gut microbiota, regulates hepatic lipogenesis and maintains lipid homeostasis via LKB1-AMPK-Insig signaling pathway. These findings also indicate that NaB mediates the crosstalk between the gut and liver in regulating metabolism, and that therapeutic approaches, such as LKB1 and Insig activators in hepatocytes, may have potential for the treatment of NAFLD and related metabolic diseases.

## **Materials and Methods**

### *Animal Model and Diets*

Male specific pathogen-free male C57BL/6 mice at 6 weeks of age were purchased from Shanghai Laboratory Animal Co. Ltd. (Shanghai, China). Mice were fed a standard chow diet or an HFD (fat 33 kcal%, carbohydrates 50 kcal%, protein 17 kcal%, and 2% cholesterol; TrophicDiet, Nantong, China)<sup>39,40</sup> for 8 weeks. Then the mice fed with HFD were randomly divided into 2 groups and treated with NaB (200 mg/kg/d) or vehicle by gavage once daily for 8 weeks. The NaB solution was prepared as previously described.<sup>20</sup> All mice were housed under a 12-hour light/dark cycle at controlled temperature. All animal experiment protocols were approved by the Institutional Animal Care and Use Committee of Xinhua hospital affiliated to Shanghai Jiao Tong University School of Medicine.

### *Histological Analysis*

Livers were fixed in 10% phosphate-buffered formalin acetate at 4°C overnight and embedded in paraffin wax. Paraffin sections (5  $\mu$ m) were cut and mounted on glass slides for hematoxylin and eosin as previously described.<sup>41</sup> Immunohistochemistry of liver sections was performed as previously described.<sup>8,19,42</sup> Liver sections were incubated with antibodies against FAS, SCD1, phosphorylated AMPK,

phosphorylated ACC, Insig-1, and Insig-2. Livers embedded in optimum cutting temperature compound (Laborimpex, Brussels, Belgium) were used for Oil Red O staining for the assessment of hepatic steatosis. The procedure was as previously described.<sup>41</sup>

### Reagents and Antibodies

Oil Red O (cat. O0625) and mouse monoclonal FLAG M2 antibody (cat. F3165) were purchased from Sigma-Aldrich (St Louis, MO). Glutathione Sepharose beads (cat. 17-0756-01) were from GE Healthcare (Piscataway, NJ). Rabbit monoclonal phospho-AMPK $\alpha$  (Thr172) antibody (1:1000, cat. 2535), rabbit monoclonal total AMPK $\alpha$  pan antibody (1:1000, cat. 2532), and mouse monoclonal Myc tag antibody (1:1000, cat. 2276) were obtained from Cell Signaling Technology (Beverly, MA). Rabbit polyclonal antibody against phospho-ACC (Ser79) (1:1000, cat. 07-303) was obtained from Merck Millipore (Billerica, MA). Total ACC (1:1000, cat. 3662) was obtained from Upstate Biotechnology (Lake Placid, NY). Mouse monoclonal FAS antibody (1:2000, cat. 610963) was from BD Biosciences (San Jose, CA). Antibodies against Insig-1 (1:500, cat. sc-390504), Insig-2 (1:500, cat. sc-66936), glutathione S-transferase (GST) (1:1000, cat. sc-138), SREBP-1 (1:1000, K10, sc-367),  $\beta$ -actin (1:2000, cat. sc-69879); horseradish peroxidase-conjugated anti-mouse (1:10,000) and anti-rabbit (1:10,000) secondary antibodies; and protein A/G PLUS-Agarose beads were obtained from Santa Cruz Biotechnology (Dallas, TX).

### Immunoblots, Co-Immunoprecipitation, and GST Pull-Down

Immunoblotting analysis was carried out as described previously.<sup>8,41,43-45</sup> In brief, mice liver tissues or cultured cells were homogenized and lysed at 4°C in lysis buffer (50 mM Tris-HCl, pH 8.0, 1% (v/v) Nonidet P-40, 150 mM NaCl, 5 mM EDTA, 1 mM EGTA, 1 mM sodium orthovanadate, 10 mM sodium fluoride, 1 mM phenylmethylsulfonyl fluoride, 2  $\mu$ g/mL aprotinin, 5  $\mu$ g/mL leupeptin, and 1  $\mu$ g/mL pepstatin). Cell lysates were centrifuged at 14,000 rpm for 10 minutes at 4°C, and the resulting supernatant was used for immunoblotting analysis. Protein concentrations in cell lysates were measured using Bio-Rad Protein Assay Dye Reagent. For immunoblotting, 20–50  $\mu$ g of protein was separated by 8%–10% sodium dodecyl sulfate polyacrylamide gel electrophoresis and then electrophoretically transferred to polyvinylidene difluoride membranes in a transfer buffer consisting of 25 mM Tris base, 190 mM glycine, and 20% methanol. The membranes were blocked with 5% nonfat milk in Tris-buffered saline with 0.1% Tween 20 and incubated with specific antibodies, followed by incubation with horseradish peroxidase-conjugated secondary antibodies. Immunoblots were visualized by LumiGLO chemiluminescence detection kit (Cell Signaling Technology). The intensity of bands was quantified using ImageJ (v1.53, National Institutes of Health, Bethesda, MD). Relative phosphorylation levels were normalized to those of endogenous proteins and presented as the mean  $\pm$  SEM. For

co-immunoprecipitation, cell lysates containing overexpressed recombinant or endogenous proteins were incubated with specific antibodies and protein A/G Sepharose beads at 4°C for overnight. The precipitates were washed 3 times with ice-cold lysis buffer. For GST pull-down analysis, cell lysates containing overexpressed GST tagged fusion proteins or endogenous proteins were incubated with Glutathione Sepharose 4B beads (GE Healthcare Bio-Sciences, Pittsburgh, PA) at 4°C overnight and washed as co-immunoprecipitation. The precipitates were then analyzed by immunoblots.

### Primary Mouse Hepatocyte Isolation and Culture

Primary mouse hepatocytes were isolated as previously described.<sup>9</sup> Briefly, 6-well plates were coated by rat-tail collagen type I (cat. 08-115; Merck Millipore) overnight, and then washed by phosphate-buffered saline twice. Briefly, mice were anesthetized with sodium pentobarbital (30 mg/kg intraperitoneally) and the portal vein was cannulated under aseptic conditions. The liver was perfused with EGTA solution (5.4 mmol/L KCl, 0.44 mmol/L KH<sub>2</sub>PO<sub>4</sub>, 140 mmol/L NaCl, 0.34 mmol/L Na<sub>2</sub>HPO<sub>4</sub>, 0.5 mmol/L EGTA, 25 mmol/L Tricine, pH 7.2) and Hank's balanced salt solution containing 0.075% collagenase type I (Sigma-Aldrich), 10 mg/mL DNase I (Sigma-Aldrich), 200 units/mL penicillin, and 200  $\mu$ g/mL streptomycin, and then digested with 0.025% collagenase solution for the mouse liver. The isolated mouse hepatocytes were then cultured at 80%–90% confluence in Dulbecco's modified Eagle medium containing 10% fetal bovine serum in rat-tail collagen type I-coated 6-well plates (BD Biosciences) overnight. Cells were infected with adenoviruses expressing Insig-1 or green fluorescent protein, treated without or with NaB in a serum-free medium.

### Cell Lines and Treatment

Human HepG2 hepatocyte and HEK293 cells were purchased from Cell Bank, Type Culture Collection Committee, Chinese Academy of Sciences (Shanghai, China). The cells were cultured, and treated as indicated. Cells were cultured in Dulbecco's modified Eagle medium containing 5.5 mM D-glucose, 10% fetal bovine serum, 100 units/mL penicillin, and 100  $\mu$ g/mL streptomycin and incubated in a humidified atmosphere of 5% CO<sub>2</sub> at 37°C and passaged every 2 days by trypsinization. Cells were transfected with plasmids for 24 hours, followed by treatment with 1–10 mM NaB for 24 hours. The cells were grown in monolayer at 37°C in 5% CO<sub>2</sub>, and were maintained in medium D. Medium D, including a 1:1 mixture of Ham's F12 medium and Dulbecco's modified Eagle's medium containing 100 units/mL penicillin, and 100  $\mu$ g/mL streptomycin, supplied 5% fetal bovine serum, 5  $\mu$ g/mL cholesterol, 1 mM sodium mevalonate, and 20  $\mu$ M sodium oleate.

### Statistical Analysis

Data are expressed as mean  $\pm$  SEM. Statistical significance was evaluated using the unpaired 2-tailed Student's *t* test and among more than 2 groups by analysis of 1-way

analysis of variance. Differences were considered significant at a  $P$  value  $<.05$ .

## References

- Fan JG, Kim SU, Wong VW. New trends on obesity and NAFLD in Asia. *J Hepatol* 2017;67:862–873.
- Paik JM, Golabi P, Younossi Y, Mishra A, Younossi ZM. Changes in the global burden of chronic liver diseases from 2012 to 2017: The growing impact of nonalcoholic fatty liver disease. *Hepatology* 2020; 72:1605–1616.
- Samuel VT, Shulman GI. Nonalcoholic fatty liver disease as a nexus of metabolic and hepatic diseases. *Cell Metab* 2018;27:22–41.
- Smith GI, Shankaran M, Yoshino M, Schweitzer GG, Chondronikola M, Beals JW, Okunade AL, Patterson BW, Nyangau E, Field T, Sirlin CB, Talukdar S, Hellerstein MK, Klein S. Insulin resistance drives hepatic de novo lipogenesis in nonalcoholic fatty liver disease. *J Clin Invest* 2020;130:1453–1460.
- Goedeke L, Bates J, Vatner DF, Perry RJ, Wang T, Ramirez R, Li L, Ellis MW, Zhang D, Wong KE, Beysen C, Cline GW, Ray AS, Shulman GI. Acetyl-CoA carboxylase inhibition reverses nafld and hepatic insulin resistance but promotes hypertriglyceridemia in rodents. *Hepatology* 2018;68:2197–2211.
- Alkhoury N, Lawitz E, Nouredin M, DeFronzo R, Shulman GI. Gs-0976 (Firsocostat): An investigational liver-directed acetyl-CoA carboxylase (ACC) inhibitor for the treatment of non-alcoholic steatohepatitis (NASH). *Expert Opin Investig Drugs* 2020;29:135–141.
- Engelking LJ, Kuriyama H, Hammer RE, Horton JD, Brown MS, Goldstein JL, Liang G. Overexpression of *insig-1* in the livers of transgenic mice inhibits *srebp* processing and reduces insulin-stimulated lipogenesis. *J Clin Invest* 2004;113:1168–1175.
- Li Y, Xu S, Mihaylova MM, Zheng B, Hou X, Jiang B, Park O, Luo Z, Lefai E, Shyy JY, Gao B, Wierzbicki M, Verbeuren TJ, Shaw RJ, Cohen RA, Zang M. Ampk phosphorylates and inhibits *srebp* activity to attenuate hepatic steatosis and atherosclerosis in diet-induced insulin-resistant mice. *Cell Metab* 2011;13:376–388.
- Han Y, Hu Z, Cui A, Liu Z, Ma F, Xue Y, Liu Y, Zhang F, Zhao Z, Yu Y, Gao J, Wei C, Li J, Fang J, Li J, Fan J-G, Song B-L, Li Y. Post-translational regulation of lipogenesis via ampk-dependent phosphorylation of insulin-induced gene. *Nat Commun* 2019;10:623.
- Shaw RJ, Lamia KA, Vasquez D, Koo SH, Bardeesy N, Depinho RA, Montminy M, Cantley LC. The kinase LKB1 mediates glucose homeostasis in liver and therapeutic effects of metformin. *Science* 2005;310:1642–1646.
- Zhao ZH, Lai JK, Qiao L, Fan JG. Role of gut microbial metabolites in nonalcoholic fatty liver disease. *J Dig Dis* 2019;20:181–188.
- Donohoe DR, Garge N, Zhang X, Sun W, O'Connell TM, Bunker MK, Bultman SJ. The microbiome and butyrate regulate energy metabolism and autophagy in the mammalian colon. *Cell Metab* 2011;13:517–526.
- Nicholson JK, Holmes E, Kinross J, Burcelin R, Gibson G, Jia W, Pettersson S. Host-gut microbiota metabolic interactions. *Science* 2012;336:1262–1267.
- Canfora EE, Jocken JW, Blaak EE. Short-chain fatty acids in control of body weight and insulin sensitivity. *Nat Rev Endocrinol* 2015;11:577–591.
- Tolhurst G, Heffron H, Lam YS, Parker HE, Habib AM, Diakogiannaki E, Cameron J, Grosse J, Reimann F, Gribble FM. Short-chain fatty acids stimulate glucagon-like peptide-1 secretion via the g-protein-coupled receptor FFAR2. *Diabetes* 2012;61:364–371.
- Furusawa Y, Obata Y, Fukuda S, Endo TA, Nakato G, Takahashi D, Nakanishi Y, Uetake C, Kato K, Kato T, Takahashi M, Fukuda NN, Murakami S, Miyauchi E, Hino S, Atarashi K, Onawa S, Fujimura Y, Lockett T, Clarke JM, Topping DL, Tomita M, Hori S, Ohara O, Morita T, Koseki H, Kikuchi J, Honda K, Hase K, Ohno H. Commensal microbe-derived butyrate induces the differentiation of colonic regulatory T cells. *Nature* 2013; 504:446–450.
- Arpaia N, Campbell C, Fan X, Dikiy S, van der Veeken J, deRoos P, Liu H, Cross JR, Pfeffer K, Coffey PJ, Rudensky AY. Metabolites produced by commensal bacteria promote peripheral regulatory T-cell generation. *Nature* 2013;504:451–455.
- Ilan Y. Review article: Novel methods for the treatment of non-alcoholic steatohepatitis - targeting the gut immune system to decrease the systemic inflammatory response without immune suppression. *Aliment Pharmacol Ther* 2016;44:1168–1182.
- Zhou D, Pan Q, Xin FZ, Zhang RN, He CX, Chen GY, Liu C, Chen YW, Fan JG. Sodium butyrate attenuates high-fat diet-induced steatohepatitis in mice by improving gut microbiota and gastrointestinal barrier. *World J Gastroenterol* 2017;23:60–75.
- Zhou D, Chen YW, Zhao ZH, Yang RX, Xin FZ, Liu XL, Pan Q, Zhou H, Fan JG. Sodium butyrate reduces high-fat diet-induced non-alcoholic steatohepatitis through upregulation of hepatic *glp-1r* expression. *Exp Mol Med* 2018;50:1–12.
- Du Y, Li X, Su C, Xi M, Zhang X, Jiang Z, Wang L, Hong B. Butyrate protects against high-fat diet-induced atherosclerosis via up-regulating *abca1* expression in apolipoprotein e-deficiency mice. *Br J Pharmacol* 2020; 177:1754–1772.
- Liu J, Wang F, Liu S, Du J, Hu X, Xiong J, Fang R, Chen W, Sun J. Sodium butyrate exerts protective effect against parkinson's disease in mice via stimulation of glucagon like peptide-1. *J Neurol Sci* 2017; 381:176–181.
- Russo R, De Caro C, Avagliano C, Cristiano C, La Rana G, Mattace Raso G, Berni Canani R, Meli R, Calignano A. Sodium butyrate and its synthetic amide derivative modulate nociceptive behaviors in mice. *Pharmacol Res* 2016;103:279–291.
- Pan X, Fang X, Wang F, Li H, Niu W, Liang W, Wu C, Li J, Tu X, Pan LL, Sun J. Butyrate ameliorates caerulein-induced acute pancreatitis and associated intestinal injury by tissue-specific mechanisms. *Br J Pharmacol* 2019;176:4446–4461.

25. Bloemen JG, Venema K, van de Poll MC, Olde Damink SW, Buurman WA, Dejong CH. Short chain fatty acids exchange across the gut and liver in humans measured at surgery. *Clin Nutr* 2009;28:657–661.
26. Bedossa P, Poitou C, Veyrie N, Bouillot JL, Basdevant A, Paradis V, Tordjman J, Clement K. Histopathological algorithm and scoring system for evaluation of liver lesions in morbidly obese patients. *Hepatology* 2012;56:1751–1759.
27. Cui A, Hu Z, Han Y, Yang Y, Li Y. Optimized analysis of in vivo and in vitro hepatic steatosis. *J Vis Exp* 2017;121:55178.
28. Woods A, Johnstone SR, Dickerson K, Leiper FC, Fryer LG, Neumann D, Schlattner U, Wallimann T, Carlson M, Carling D. Lkb1 is the upstream kinase in the amp-activated protein kinase cascade. *Curr Biol* 2003;13:2004–2008.
29. Gowans GJ, Hawley SA, Ross FA, Hardie DG. Amp is a true physiological regulator of amp-activated protein kinase by both allosteric activation and enhancing net phosphorylation. *Cell Metab* 2013;18:556–566.
30. Stephenne X, Foretz M, Taleux N, van der Zon GC, Sokal E, Hue L, Viollet B, Guigas B. Metformin activates amp-activated protein kinase in primary human hepatocytes by decreasing cellular energy status. *Diabetologia* 2011;54:3101–3110.
31. Sun Y, Yuan X, Zhang F, Han Y, Chang X, Xu X, Li Y, Gao X. Berberine ameliorates fatty acid-induced oxidative stress in human hepatoma cells. *Sci Rep* 2017;7:11340.
32. Henagan TM, Stefanska B, Fang Z, Navard AM, Ye J, Lenard NR, Devarshi PP. Sodium butyrate epigenetically modulates high-fat diet-induced skeletal muscle mitochondrial adaptation, obesity and insulin resistance through nucleosome positioning. *Br J Pharmacol* 2015;172:2782–2798.
33. Aguilar EC, Santos LC, Leonel AJ, de Oliveira JS, Santos EA, Navia-Pelaez JM, da Silva JF, Mendes BP, Capettini LS, Teixeira LG, Lemos VS, Alvarez-Leite JI. Oral butyrate reduces oxidative stress in atherosclerotic lesion sites by a mechanism involving nadph oxidase down-regulation in endothelial cells. *J Nutr Biochem* 2016;34:99–105.
34. Yang W, Yu T, Huang X, Bilotta AJ, Xu L, Lu Y, Sun J, Pan F, Zhou J, Zhang W, Yao S, Maynard CL, Singh N, Dann SM, Liu Z, Cong Y. Intestinal microbiota-derived short-chain fatty acids regulation of immune cell il-22 production and gut immunity. *Nat Commun* 2020;11:4457.
35. Li Z, Yi CX, Katiraei S, Kooijman S, Zhou E, Chung CK, Gao Y, van den Heuvel JK, Meijer OC, Berbee JFP, Heijink M, Giera M, Willems van Dijk K, Groen AK, Rensen PCN, Wang Y. Butyrate reduces appetite and activates brown adipose tissue via the gut-brain neural circuit. *Gut* 2018;67:1269–1279.
36. Xu D, Wang Z, Xia Y, Shao F, Xia W, Wei Y, Li X, Qian X, Lee JH, Du L, Zheng Y, Lv G, Leu JS, Wang H, Xing D, Liang T, Hung MC, Lu Z. The gluconeogenic enzyme pck1 phosphorylates insig1/2 for lipogenesis. *Nature* 2020;580:530–535.
37. Tong X, Christian P, Zhao M, Wang H, Moreau R, Su Q. Activation of hepatic crebh and insig signaling in the anti-hypertriglyceridemic mechanism of r-alpha-lipoic acid. *J Nutr Biochem* 2015;26:921–928.
38. Tang M, Floyd S, Cai H, Zhang M, Yang R, Dang R. The status of omega-3 pufas influence chronic unpredicted mild stress-induced metabolic side effects in rats through insig/srebp pathway. *Food Funct* 2019;10:4649–4660.
39. Fan JG, Zhong L, Xu ZJ, Tia LY, Ding XD, Li MS, Wang GL. Effects of low-calorie diet on steatohepatitis in rats with obesity and hyperlipidemia. *World J Gastroenterol* 2003;9:2045–2049.
40. Fan JG, Xu ZJ, Wang GL. Effect of lactulose on establishment of a rat non-alcoholic steatohepatitis model. *World J Gastroenterol* 2005;11:5053–5056.
41. Zhang F, Hu Z, Li G, Huo S, Ma F, Cui A, Xue Y, Han Y, Gong Q, Gao J, Bian H, Meng Z, Wu H, Long G, Tan Y, Zhang Y, Lin X, Gao X, Xu A, Li Y. Hepatic crebzf couples insulin to lipogenesis by inhibiting insig activity and contributes to hepatic steatosis in diet-induced insulin-resistant mice. *Hepatology* 2018;68:1361–1375.
42. Zhao ZH, Xin FZ, Xue Y, Hu Z, Han Y, Ma F, Zhou D, Liu XL, Cui A, Liu Z, Liu Y, Gao J, Pan Q, Li Y, Fan JG. Indole-3-propionic acid inhibits gut dysbiosis and endotoxin leakage to attenuate steatohepatitis in rats. *Exp Mol Med* 2019;51:1–14.
43. Gong Q, Hu Z, Zhang F, Cui A, Chen X, Jiang H, Gao J, Chen X, Han Y, Liang Q, Ye D, Shi L, Chin YE, Wang Y, Xiao H, Guo F, Liu Y, Zang M, Xu A, Li Y. Fibroblast growth factor 21 improves hepatic insulin sensitivity by inhibiting mammalian target of rapamycin complex 1 in mice. *Hepatology* 2016;64:425–438.
44. Chen X, Zhang F, Gong Q, Cui A, Zhuo S, Hu Z, Han Y, Gao J, Sun Y, Liu Z, Yang Z, Le Y, Gao X, Dong LQ, Gao X, Li Y. Hepatic atf6 increases fatty acid oxidation to attenuate hepatic steatosis in mice through peroxisome proliferator-activated receptor alpha. *Diabetes* 2016;65:1904–1915.
45. Hu Z, Han Y, Liu Y, Zhao Z, Ma F, Cui A, Zhang F, Liu Z, Xue Y, Bai J, Wu H, Bian H, Chin YE, Yu Y, Meng Z, Wang H, Liu Y, Fan J, Gao X, Chen Y, Li Y. Crebzf as a key regulator of stat3 pathway in the control of liver regeneration in mice. *Hepatology* 2020;71:1421–1436.

---

Received January 26, 2021. Accepted May 5, 2021.

#### Correspondence

Address correspondence to Yu Li, PhD, Shanghai Institute of Nutrition and Health, Chinese Academy of Sciences, 320 Yue Yang Road, Life Science Research Building A1816, Shanghai 200031, China. e-mail: fanjiangao@xinhumed.com.cn; OR Jian-Gao Fan, PhD, Center for Fatty Liver, Department of Gastroenterology, Xinhua Hospital Affiliated to Shanghai Jiao Tong University School of Medicine, Shanghai Key Lab of Pediatric Gastroenterology and Nutrition, 1665 Kong Jiang Road, Shanghai 200092, China. e-mail: liyu@sibs.ac.cn.

#### Acknowledgments

The authors thank Drs. Daming Gao and Hongbin Ji (Shanghai Institute of Biochemistry and Cell Biology, Chinese Academy of Sciences) for providing LKB1-deficient MEF cells, Drs. Jingya Li and Jia Li (Shanghai Institute of Materia Medica, Chinese Academy of Sciences) for providing floxed AMPK  $\alpha 1/\alpha 2$  double knockout (AMPK $^{-/-}$ ) mice, and Lili Zhang and Yin Li (Shanghai Institute of Nutrition and Health, Chinese Academy of Sciences) for technical assistance.

**CRedit Authorship Contributions**

Ze-Hua Zhao, PhD (Funding acquisition: Supporting; Investigation: Equal; Writing – original draft: Lead)  
 Zi-Xuan Wang (Investigation: Equal; Writing – original draft: Supporting)  
 Da Zhou, PhD (Investigation: Supporting)  
 Yamei Han, PhD (Investigation: Supporting)  
 Fengguang Ma (Investigation: Supporting)  
 Zhimin Hu, PhD (Investigation: Supporting)  
 Feng-Zhi Xin, PhD (Investigation: Supporting)  
 Xiao-Lin Liu, PhD (Investigation: Supporting)  
 Tian-Yi Ren, PhD (Investigation: Supporting; Methodology: Supporting)  
 Feifei Zhang, PhD (Investigation: Supporting)  
 Yaqian Xue (Investigation: Supporting)  
 Aoyuan Cui, PhD (Investigation: Supporting)  
 Zhengshuai Liu (Investigation: Supporting)  
 Jinyun Bai, PhD (Investigation: Supporting)  
 Yuxiao Liu (Investigation: Supporting)  
 Genxiang Cai (Investigation: Supporting)  
 Weitong Su (Investigation: Supporting)  
 Xiaozhen Dai, PhD (Writing – review & editing: Supporting)  
 Feng Shen, PhD (Supervision: Supporting)  
 Qin Pan, PhD (Supervision: Supporting)

Yu Li, PhD (Conceptualization: Equal; Funding acquisition: Equal; Projectadministration: Equal; Supervision: Equal; Validation: Equal; Writing – review & editing: Equal)

Jian-Gao Fan, MD (Conceptualization: Equal; Funding acquisition: Equal; Projectadministration: Equal; Supervision: Equal; Validation: Equal; Writing – review & editing: Equal)

**Conflicts of interest**

The authors disclose no conflicts.

**Funding**

This work was supported by the National Key R&D Program of China (2017YFC0908903) and the National Natural Science Foundation of China (81873565, 81470840, and 81600464) to Jian-Gao Fan. This work was also supported by grants from the National Key R&D Program of China (2019YFA0802502), the National Natural Science Foundation of China (81925008), the Key Laboratory of Wuliangye-flavor Liquor Solid-state Fermentation of China National Light Industry (2019JJ005), and the Shanghai Science and Technology Commission (19140903300) to Yu Li; and by a grant from the National Natural Science Foundation of China (82000542) to Ze-Hua Zhao.